Review

Not peer-reviewed version

Recent Advances of Single-atom Metal Supported at Two-dimensional MoS2 for Electrochemical CO2 Reduction and Water Splitting

Jiahao Wang , Xiaorong Gan * , Tianhao Zhu , Dan Zhao , Yanhui Ao , Peifang Wang

Posted Date: 29 August 2023

doi: 10.20944/preprints202308.1932.v1

Keywords: single-atom metal; two-dimensional nanomaterials; water splitting; CO2 reduction; catalysis; DFT

Review

Recent Advances of Single-Atom Metal Supported at Two-Dimensional MoS_2 for Electrochemical CO_2 Reduction and Water Splitting

Jiahao Wang [1], Xiaorong Gan [1,2,*], Tianhao Zhu [3], Dan Zhao [4], Yanhui Ao [1] and Peifang Wang [1]

[1] Key Laboratory of Integrated Regulation and Resource Development on Shallow Lake of Ministry of Education, College of Environment, Hohai University, Nanjing 210098, China;
[2] Key Lab of Modern Optical Technologies of Jiangsu Province, Soochow University, Suzhou 215006, China;
[3] Department of Civil and Environmental Engineering, University of Michigan, Ann Arbor, MI 48109 USA;
[4] Department of Clinical Laboratory Medicine, Xijing Hospital, AirForce military medical university, Xi'an, Shaanxi, China;
* Correspondence: gumphope@hhu.edu.cn

Abstract: Due to increasing concerns about global warming and energy crisis, intensive efforts have been made to explore renewable and clean energy sources. Single-atom metals and two-dimensional (2D) nanomaterials have attracted extensive attention in the fields of energy and environment because of their unique electronic structures and excellent properties. In this review, we summarize the state-of-art progress on the single-atom metal supported at 2D MoS_2 (single-atom metal/2D MoS_2) for electrochemical CO_2 reduction and water splitting. First, we introduce the advantages of single-atom metal/2D MoS_2 catalysts in the fields of electrocatalytic CO_2 reduction and water splitting, followed by the strategies for improving electrocatalytic performances of single-atom metal/2D MoS_2 hybrid nanomaterials and the typical preparation methods. Further, we discuss the important applications of the nanocomposites in electrocatalytic CO_2 reduction and water splitting via some typical examples, particularly focusing on their synthesis routes, modification approaches, and physiochemical mechanisms for improving their electrocatalytic performances. Finally, our perspectives on the key challenges and future directions of exploring high-performance metal single-atom catalysts are presented based on recent achievements in the development of single-atom metal/2D MoS_2 hybrid nanomaterials.

Keywords: single-atom metal; two-dimensional nanomaterials; water splitting; CO_2 reduction; catalysis; DFT

1. Introduction

Due to the contamination and global warming problems, it is necessary to search for alternative environmentally friendly energy sources and decrease the concentration of CO_2 in the atmosphere [1-3]. The utilization of nonprecious metal electrocatalysts for water splitting and CO_2 fixation for producing high value-added fuels or chemicals may be the ultimate solution for sustainable and clean hydrogen energy and tackling the challenges posed by rising CO_2 levels and realizing a closed carbon cycle [4]. However, electrocatalysts for CO_2 reduction reaction (CO_2RR) and water splitting face some problems, such as low product selectivity, poor faradaic efficiency (FE), and/or hard experimental conditions (in acidic media) [5,6]. In particular, the catalytic activity and selectivity of non-precious metal catalysts are generally much lower than those of noble metal catalysts [7]. The activity of catalysts is not only related to the composition and structure, but also to the dimension or size. The most direct effect of the decrease in dimension or size is the change in the number of active sites. Compared with conventional nanoparticles, single-atom catalysts (SACs) have the advantages of unique electronic structure, strong metal-support interactions (SMSIs), and plenty of accessible active

 doi:10.20944/preprints202308.1932.v1

sites, and thus can significantly improve catalytic activity and selectivity [8-10]. Therefore, SACs have shown prominent activity in various electrochemistry processes including CO_2RR [11,12], oxygen evolution reaction (OER) [13,14], and hydrogen evolution reaction (HER) [15,16]. However, since the surface energy increases with the decrease of particle size, the single atoms tend to aggregate into clusters or nanoparticles [17,18], which leads to the degraded functions. Hence, it is indispensable to anchor the isolated atoms onto the appropriate supports to build the stable configurations with atomic distribution [19,20]. On the one hand, these supports can serve for stabilizing functions [21]. The strong metal-support interactions can effectively tune the electronic structure of SACs to improve the electrocatalytic activity and selectivity [22-24]. 2D materials are recognized as ideal supports for SACs and the preferable alternatives for catalysts due to their unique electronic properties, high specific surface area, and substantial number of active sites [25-28]. For example, Mn supported on 2D VTe_2 exhibits excellent catalytic performance for both HER and OER [29]. Recent advances have demonstrated that 2D materials can improve the performance of SACs and the inhomogeneity of active sites [30-32].

2D molybdenum disulfide (MoS_2) as the representative of transition metal dichalcogenides (TMDCs), has attracted much attention for HER, OER and CO_2RR due to its unique structure and ability to be chemically modified [33,34]. Owing to the high earth abundance, low price and high HER catalytic activity, 2D MoS_2 is regarded as a promising catalyst, compared with noble metal, for water splitting [35]. In addition, 2D MoS_2 has a great potential electrocatalyst for CO_2RR because Mo-exposed edges can enhance the chemisorption of the reactants, and thus improve the electrochemical catalysis with a low overpotential of CO_2RR (about ~54 mV) and high selectivity (the reduction product is only CO) [34,36]. However, the electrocatalytic performance of pristine 2D MoS_2 is still not satisfactory. For example, MoS_2 edges show poor oxygen evolution reaction (OER) activity [37] and the pristine basal plane of MoS_2 is inert to electrochemical reduction of CO_2 [38]. In contrast, Therefore, the successful combination of 2D MoS_2 and single-atom metal may remedy their respective shortcomings and increase the active sites, surface area and electronic conductivity, ultimately enhancing electrocatalytic CO_2RR and overall water splitting.

Recently, single-atom metal/2D MoS_2 hybrid nanomaterials have been booming in heterogeneous catalysis, especially electrocatalysis, due to their well-defined, precisely located metal centers, unique metal–support interaction, and identical coordination environment. However, there have been only a few studies on the systematic summarization of the nanomaterials for electrocatalytic CO_2RR and overall water splitting. Thus, to fill this gap, a comprehensive review on such a topic is extremely necessary and significant. In this review, we summarize the state-of-art progress on single-atom metal nanomaterials modified 2D MoS_2 for electrocatalytic CO_2RR and water splitting. We start briefly from a discussion of the unique advantages of single-atom metal/2D MoS_2 hybrid nanomaterials for electrocatalytic CO_2RR and water splitting. Further, the synthetic methods for single-atom metal/2D MoS_2 hybrid nanomaterials are summarized, including one-pot chemical method, electrochemical process, and polyoxometalate template-based synthetic strategy. After that, we highlight the significant applications of single-atom metal/2D MoS_2 hybrid nanomaterials in electrocatalytic CO_2RR and water splitting, particularly focusing on physiochemical mechanisms for improving their electrocatalytic activity. Finally, on the basis of previous studies, we provide our perspectives on the key challenges and future directions in utilizing single-atom metal/2D MoS_2 hybrid nanomaterials for CO_2RR and water splitting. We hope that this review can provide new insights for the further development and practical application of single-atom catalysts and 2D materials.

2. Synthesis Methods of Hybrid Nanomaterials

The catalytic performances are determined by concrete improvements of synthetic methodologies [39]. The most widely employed approaches for SACs are pyrolysis, atomic layer deposition (ALD) method, physical vapor deposition (PVD), wet-chemistry strategy, and electronic deposition [40-42]. However, it is still hard to manipulate atoms in a highly accurate way for the synthesis of theoretically designed SACs due to ultrahigh surface free energy. The synthesis

Preprints (www.preprints.org) | NOT PEER-REVIEWED | Posted: 29 August 2023 doi:10.20944/preprints202308.1932.v1

methodologies for 2D MoS_2 can be divided into two categories: top-down and bottom-up methods. The former mainly includes chemical vapor deposition (CVD) and solvothermal or hydrothermal methods [43-47]; the latter includes mechanical exfoliation, chemical or electrochemical exfoliation methods, and liquid-phase exfoliation [48]. However, the number of successful cases for single-atom metal/2D MoS_2 hybrid nanomaterials is still limited compared to the synthesis methods for single-atom metal modified 3D supports, SACs preparation, and/or 2D materials. The methods for single-atom metal/2D MoS_2 hybrid nanomaterials are derived from the approaches for SAC@3D supports such as pyrolysis and coprecipitation. Considering that the common synthetic methods of SACs or 2D materials have been discussed in depth in previous reviews, this review focuses on some novel methods for single-atom metal/2D MoS_2 hybrid nanomaterials including one-pot chemical method, electrochemical process, and polyoxometalate template-based synthetic strategy, for single-atom metal/2D MoS_2 hybrid nanomaterials (Figure 1).

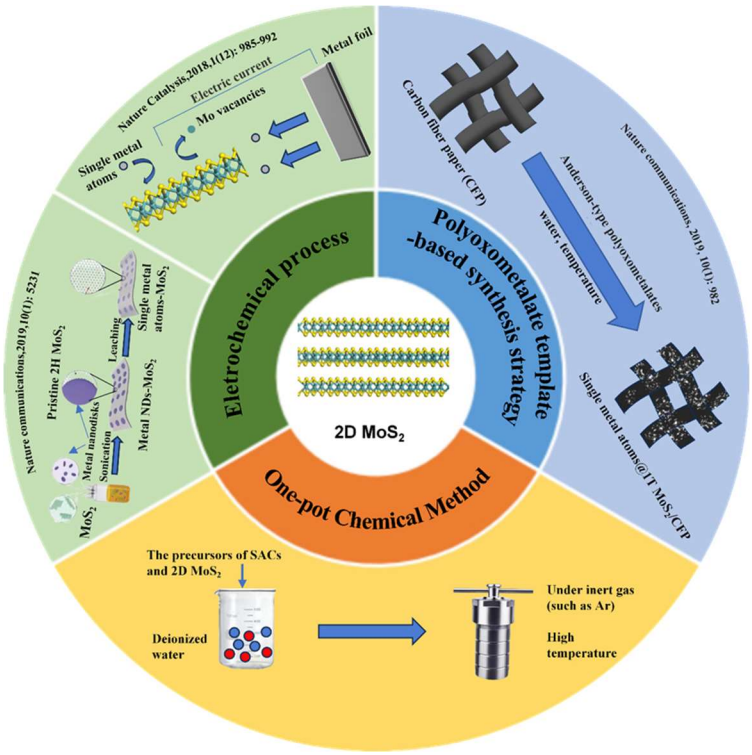

Figure 1. Several common synthesis methods of single-atom metal/2D MoS_2 hybrid nanomaterials.

2.1. One-pot Chemical Method

The principle of this method is directly to mix the precursors of SACs and 2D MoS_2 for the following reactions under inert gas (e.g., Ar). The typical processes are described as follows, firstly, all precursors (e.g., $(NH_4)_6Mo_7O_{24}{\cdot}4H_2O$, H_2PtCl_6, and CS_2) are dissolved in a certain amount of deionized water to form a homogeneous solution [15]. Then, the resulting solution is transferred to a Teflon-lined stainless autoclave under Ar and maintained at a high temperature for a certain reaction time.

One-pot method has the advantages of simple operation and saving synthetic costs. In addition, the catalysts prepared by this method can have sulfur vacancies and the doping features of metal atoms at the same time [49]. Until now, Cu@1T-MoS_2, Ni@1T-MoS_2, Fe@1T-MoS_2, and Co@1T-MoS_2 have been easily prepared through this method [50].

2.2. Electrochemical Process

Electrochemical process is used to synthesize SACs modified 2D MoS_2 via electrochemical etching of big-size metal precursor. Taking the single-atom cobalt (Co) array modified 2D MoS_2 as an example (Figure 2), firstly 2D MoS_2 and Co nanodisks (NDs) are synthesized using standard

Preprints (www.preprints.org) | NOT PEER-REVIEWED | Posted: 29 August 2023 doi:10.20944/preprints202308.1932.v1

solvothermal procedures and standard air-free procedures, respectively. Then, the combination of Co NDs and 2D MoS_2 is realized via an assembly process. Finally, single-atom Co array covalently bound onto distorted 1T-MoS_2 nanosheets (denoted as SA Co-D 1T-MoS_2) via Co-S bonds can be synthesized through electrochemical cyclic voltammetry (CV) leaching of Co nanodisks (NDs)-MoS_2 nanosheet hybrids. In addition to electrochemical CV leaching, the electrochemical deposition can be used to synthesize the nanocomposites of SACs modified 2D MoS_2, such as Pt, Cu, Sn, and Pd anchored on the 2D MoS_2, because these single metal atoms (from metal ions in the electrolyte solution) can be introduced onto the MoS_2 monolayer driven by applying the bias potential [51].

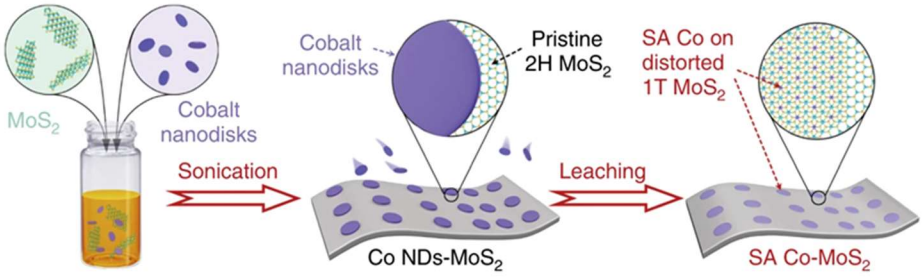

Figure 2. Schematic illustration of synthetic method for Co@1T-MoS_2. Reproduced with permission from ref [52]. Copyright 2019 Nature Communications.

2.3. Polyoxometalate Template-based Synthetic Strategy

Highly purified and stable metallic 1T-MoS_2 can be obtained by a hydrothermal method, which introduces organic sulfur sources into $(NH_4)_6Mo_7O_{24}{\cdot}4H_2O$ (denoted as Mo_7). Here, Mo_7 is a precursor that is a butterfly-shaped metal oxide cluster (Figure 3), and it belongs to the β-isomer of Anderson-type polyoxometalates (POMs). In addition, its unique structure makes it possible to tune the chemical environment of 1T-MoS_2 with various metal atoms. Using Anderson-type polyoxometalates ($[XH_6Mo_6O_{24}]^{n-}$) as precursors, atomically designing metal doping sites onto metallic 1T-MoS_2 can be achieved. $[XH_6Mo_6O_{24}]^{n-}$ is denoted as XMo_6 (X = Fe^{III}, Co^{III}, n = 3; X = Ni^{II}, n = 4) [53].

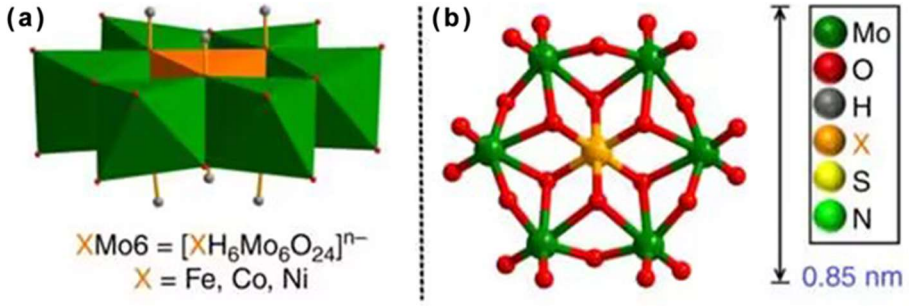

Figure 3. Structure of POM precursors. (**a**) Polyhedral representation of the XMo_6 precursors. (**b**) Ball and stick representation of the XMo_6 precursors. Reproduced with permission from ref [53]. Copyright 2019 Nature communications.

3. Single-atom Metal/2D MoS_2 Hybrid Nanomaterials for Electrochemical CO_2 Reduction

3.1. Noble Metal Modified 2D MoS_2

Electrocatalytic CO_2RR includes three steps, namely, the chemisorption of CO_2 on the surface of electrocatalysts, the transfer of high-energy electrons and protons between two elements to break C=O bonds, and the desorption of products from the surface of the electrocatalysts [54]. Noble metal single-atom catalysts (NMSACs) have the advantages of high intrinsic activity, selectivity, and durability for electrocatalytic CO_2RR due to their unique electronic structure [55]. On the other hand, in addition to acting as catalytic centers, monodispersed single noble metal atoms can also activate inert in-plane S-atoms, and lead to the improved electrochemical activity of 2D MoS_2 [56]. Compared

Preprints (www.preprints.org) | NOT PEER-REVIEWED | Posted: 29 August 2023 doi:10.20944/preprints202308.1932.v1

with the bulk MoS_2, 2D MoS_2 doped with a single-atom noble metal has the advantage of tunable electronic structures and spatial versatilities, exhibiting excellent performance in electrocatalytic CO_2RR [57]. In addition, these nanocomposites in experimental studies are usually prepared by standard electrochemical methods, which can accurately adjust the concentration of anchored single atoms by deposition time and anode voltage [58], and limiting potentials are usually used to evaluate the electrocatalytic activity of CO_2RR [11,59]. Up to now, there are few experimental studies on single-atom metal/2D MoS_2 hybrid nanomaterials for electrocatalytic CO_2RR; in contrast, a large amount of studies are focused on density functional theory (DFT) calculations for evaluating the electroactivity of single-atom metal/2D MoS_2 hybrid catalysts (as shown in Table 1). In the hybrid electrocatalysts, these single atoms in DFT calculations are mainly concentrated in Pt, Pd, Au, Ag, and Ru and have an optimal loading amount for avoiding the adverse effects on their performance. For example, single Pt atoms can introduce deep gap states, which leads to the decrease of the Fermi level upshifting and strong binding with COOH* [58]. The Ru doping can improve the H_2 adsorption and dissociation, avoiding the competing HER [60]. Moreover, because key intermediate *HCOO plays an important role in reaction pathway and potential determining steps (PDS) [61], the binding energy ($\Delta E_{Binding}$) of *HCOO on 2D MoS_2 or single-atom metal as a substrate is identified as the effective reactivity descriptor to in theory calculations. Binding energy ($\Delta E_{Binding}$) has been calculated using the following expression,

$$\Delta E_{Binding} = E_{Total} - (E_{Intermediates} + E_{Substrate})$$

where E_{Total} is the total DFT energy for the complex of intermediates (e.g., *HCOO) absorbed on a substrate (e.g., 2D MoS_2 or single metal atom), $E_{Intermediates}$ is the DFT energy for the intermediates, and $E_{Substrate}$ is the DFT energy for a substrate. The promising dopants should enhance the CO_2 and *HCOO adsorption and meanwhile weaken the CO adsorption. In addition, the binding strength can be described by the energy of the center of the d states relative to the Fermi level according to the d-band center model. In general, the high d-band center in energy relative to the Fermi level means the strong CO adsorption.

Table 1. Summary of various single-atom metal supported at 2D MoS_2 for electrochemical CO_2 reduction.

Catalyst	Potential determining steps	Limiting potentials（V）	Overpotential （V）	Production for catalysts	Ref.
Fe@MoS_2	*HCOO → *HCOOH	−0.39	0.56	CH_4	[68]
Co@MoS_2	*HCOO → *HCOOH	−0.24	0.41	CH_4	[68]
Ni@MoS_2	CO_2 → *HCOO	−0.45	0.62	CH_4	[68]
Cu@MoS_2	*OCH_3 → CH_4+*O	−1.05	1.22	CH_4	[68]

Preprints (www.preprints.org) | NOT PEER-REVIEWED | Posted: 29 August 2023 doi:10.20944/preprints202308.1932.v1

Ru@MoS_2	*CO → *CHO	−0.73	0.90	CH_4	[72]
Pd@MoS_2	CO_2 → *HCOO	−0.96	1.13	CH_4	[61]
Pt@MoS_2	CO_2 → *HCOO	−0.50	0.67	CH_4	[61]

Chemical doping with heteroatoms or surface decorating is one of the promising approaches to modulate the electronic and CO_2RR of 2D MoS_2. Proper dopants can enhance the CO_2 and COOH adsorption and meanwhile weaken the CO adsorption. Mao et al. investigated 29 kinds of single-atom metals (including Ag, Au, and other transition metal (TM) atoms) doped 2D MoS_2 with different doping concentrations and positions for electrochemical CO_2RR via high-throughput density functional theory (DFT) calculations (Figure 4a) for understanding the relationship between the doping elements and the catalytic performance [62]. For single noble metal atom doping, the binding energies of CO_2 and COOH on the Pt- and Pd-doped MoS_2 edge are greatly larger than that of the TM-doped MoS_2 (Figure 4b and Figure 4c) or pristine MoS_2; meanwhile, the binding energies of CO on Pt- and Pd-doped MoS_2 is much smaller than other TM-doped MoS_2, except for Ni-doped MoS_2. The stronger adsorption of CO_2 and COOH with MoS_2 edge can activate the reduction reaction, while the weaker adsorption of CO with MoS_2 could accelerate the rate-limiting step of CO desorption.

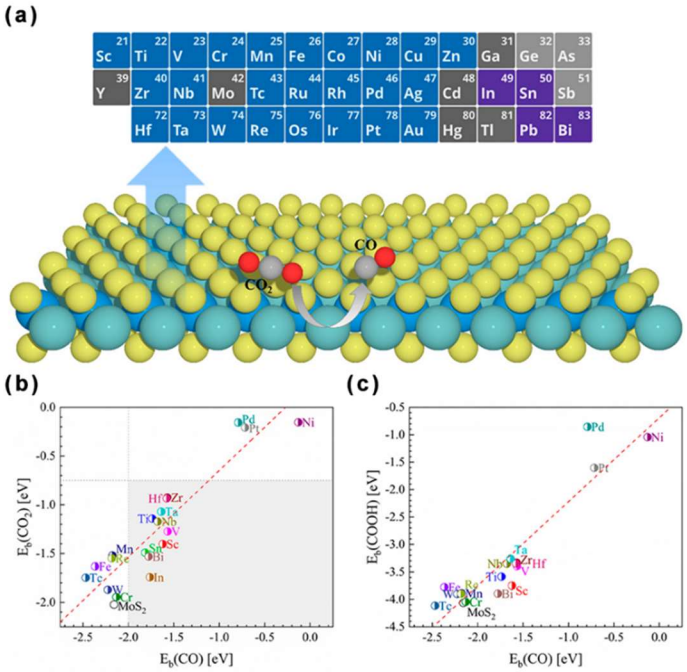

Figure 4. (**a**) 29 kinds of metals doping elements in MoS_2 as the calculation models for electrochemical CO_2RR. (**b**) Binding energies of CO_2 vs CO on the metal-doped MoS_2 edge. The gray rectangular area indicates the obvious decrease of CO binding energies. (**c**) Binding energies of COOH vs CO on the metal-doped MoS_2 edge. Reproduced with permission from ref [62]. Copyright 2020 The Journal of Physical Chemistry C.

Atomic level electroplating can accurately control the doping level and anchoring sites to maximize the activity and stability of the catalyst [58]. Xuan et. al developed an electroplating method to synthesize monodispersed noble metal atoms on 2D MoS_2 [58]. To be specific, authors demonstrated a voltage gauged electrochemical deposition method to deposit single-atom Pt, Au,

Preprints (www.preprints.org) | NOT PEER-REVIEWED | Posted: 29 August 2023 doi:10.20944/preprints202308.1932.v1

and Pd on 2D MoS_2. The surface atomic doping level for Pt, Au, and Pd can reach 1.1, 7.0, and 14 at.%, respectively, and the doping positions were accurately located on Mo- and S-vacancies. With the doping of Pt atoms, Pt, Mo and S atoms are homogeneously distributed on the MoS_2 flake (Figure 5a-d). After doping single-atom metal on 2D MoS_2, the electrochemical reactivity of the catalyst is driven higher than that of the pristine MoS_2 flakes (Figure 5e). In addition, monodisperse precious metal atoms can exhibit improved saturated CO tolerance (Figure 5f) and provide an extra pathway for CO_2RR. The overpotential of Pt-2D MoS_2 at 10 mA cm^2 only changes 9 mV after CO poisoning (Figure 5f), indicating that Pt-2D MoS_2 is almost immune to CO poisoning. Thus, due to this CO tolerance, Pt-2D MoS_2 electrocatalyst has more potential to be applied in electrocatalytic CO_2RR than Au-2D MoS_2 and Ag-2D MoS_2. The enhanced electrochemical performance is attributed to stabilized Pt (II) atoms with fewer free electrons to coordinate with CO than Pt^0 [63]. It is believed that these findings can help the non-noble single-atom doping, especially the transitional metal, and be potentially realized within fine-tuned electrochemical windows.

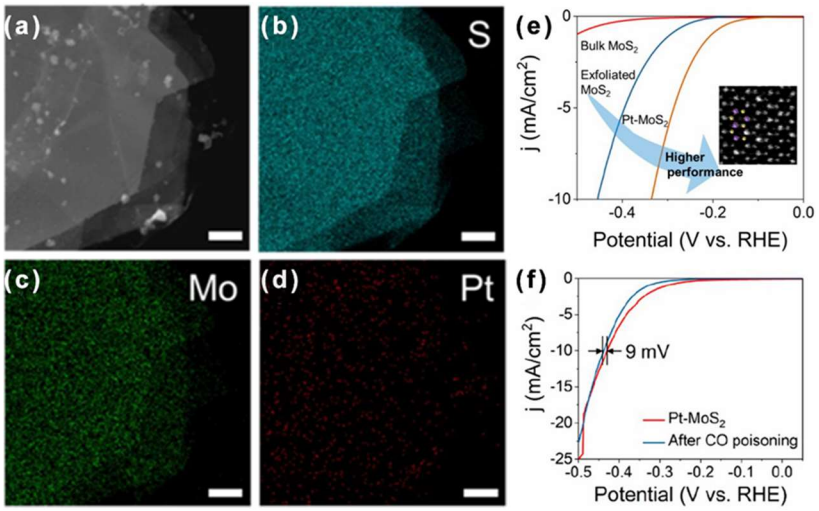

Figure 5. (**a-d**) HAADF-STEM image and corresponding EDX mapping images of Pt-MoS_2. (**e**) Single-atom electroplating process related polarization curves, from bulk MoS_2, exfoliated MoS_2/GP, and Pt-MoS_2 electrode. (**f**) CO tolerance test of Pt-2H-MoS_2 catalyst in CO saturated 0.5 M H_2SO_4. Reproduced with permission from ref [58]. Copyright 2018 Chemistry of Materials.

3.2. Non-noble Metal Modified 2D MoS_2

Exploring MoS_2-based non-noble metal SACs for electrocatalytic CO_2RR is expected to solve the problems of high overpotential, low Faraday efficiency, and unsatisfactory selectivity in CO_2RR [64]. The geometric, electronic, spin states of the active center and magnetic states of transition metal SACs can be fine-tuned to determine the catalytic behavior and activity, which can help SACs be precisely designed with 2D MoS_2 as a support to improve electronic conductivity and increase the exposed active sites for electrocatalytic CO_2RR [65]. Moreover, the TM atoms doping can significantly modify the binding energies of intermediates (e.g., *COOH) on 2D MoS_2 edges, and thus regulate the electrocatalytic performance for CO_2RR [66]. Remarkably, in addition to the ability of changing the binding energies of key intermediates, non-noble metal single-atom catalysts also have high CO formation turnover frequency (TOF), which makes it possible for their electrocatalytic performance to surpass that of NMSACs. For example, it has been proved that Nb-doped 2D MoS_2 shows 2 orders of magnitude higher CO formation TOF than Ag-doped 2D MoS_2 at an overpotential range of 100–650 mV [67].

Yu et al. used the first principles quantum theory to explore the stabilities of SACs with the non-noble 3d-series of metal single atoms (Sc, Ti, V, Cr, Mn, Fe, Co, Ni, Cu, Zn) supported on 2D MoS_2 [68]. Among them, Ni@MoS_2 is the most stable SAC, which has been proved by the analysis results including electron localization function (ELF), density of states (DOS), and band structure. All these enhancements of electrocatalytic performance for CO_2RR are attributed to the changes of the spin

Preprints (www.preprints.org) | NOT PEER-REVIEWED | Posted: 29 August 2023 doi:10.20944/preprints202308.1932.v1

densities and charge density difference by Ni doping, and thus can improve the electrocatalytic performance for CO_2RR. To supplement the theoretical and experimental gaps in the single-atom metal catalysts on 2D MoS_2 toward CO_2RR, Ren et al. explored single atom (Fe, Co, Ni, Cu) supported on 2D MoS_2 for their CO_2RR performance by the combination of DFT calculations and computational hydrogen electrode (CHE) model [69]. The limiting potentials of Fe@MoS_2, Co@MoS_2, and Ni@MoS_2 are determined as −0.39 V, −0.24 V, and −0.45 V, respectively, for CH_4 production. The binding energy of *HCOO was regarded as an effective descriptor to screen potential active single-atom catalysts for CO_2RR [61].

The endothermic and rate-limiting CO desorption step largely limited the electrocatalytic CO_2RR performance of 2D MoS_2 [70]. Nb@2D MoS_2 had a high CO formation TOF and an extremely low onset overpotential (31 mV) for electrocatalytic CO_2RR because low Nb doping concentrations (<~5%) can reduce the binding energies between intermediates and MoS_2 edge atoms [67]. Energy dispersive spectroscopy (EDS) mapping (Figure 6a) demonstrates that the distribution of Nb is homogeneous in the VA (vertically aligned)-$Mo_{0.95}Nb_{0.05}S_2$ structure. The changes of doping percentage will affect the electrocatalytic performance of Nb@2D MoS_2. When the doping percentage is 5%, the current density of Nb@2D MoS_2 is the highest (Figure 6b) and the overpotential is the lowest (Figure 6c), indicating that VA-$Mo_{0.95}Nb_{0.05}S_2$ has the best electrocatalytic performance for CO_2RR, far exceeding that of the pristine MoS_2 or Ta@2D MoS_2, because Nb doping can reduce the bonding strength between Mo edge and CO, and Nb@2D MoS_2 can result in a faster turnover for CO desorption than pristine MoS_2. However, a higher Nb doping percentage will bring about poor electron-transfer properties for CO_2RR. VA-$Mo_{0.95}Nb_{0.05}S_2$ generates a tunable mixture of CO and H_2 ranging from 12% to 82% of CO formation at the range of studied potentials −0.16 to −0.8 V (Figure 6d). At the low overpotential range of 0–150 mV, the overall electrocatalytic performance of VA-$Mo_{0.95}Nb_{0.05}S_2$ is one order of magnitude higher than that of the pristine VA-MoS_2 [71]. The electrocatalytic activity of VA-$Mo_{0.95}Nb_{0.05}S_2$ catalyst is also 2 orders of magnitude better than Ag NPs catalyst over the entire range of overpotentials (Figure 6e). The enhancement of electrocatalytic performance is due to the change of electronic properties of edge atoms by Nb doping.

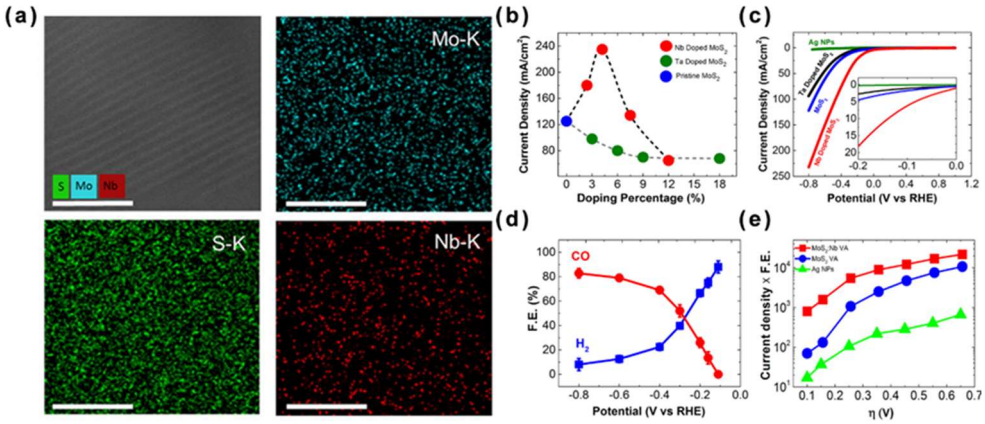

Figure 6. (**a**) EDS maps Mo–K series, Nb–K series, and S–K series measured from the same region of the MoS_2: Nb sample. (**b**) Current density as a function of dopant percentage for Nb-doped and Ta-doped MoS_2 samples. (**c**) CV curves for Ag NPs, VA-MoS_2, VA-$Mo_{0.97}Ta_{0.03}S_2$, and VA-$Mo_{0.95}Nb_{0.05}S_2$ in CO_2 environment. (**d**) CO and H_2 Faradaic efficiency (FE%) at different applied potentials for VA-$Mo_{0.95}Nb_{0.05}S_2$. (**e**) CO formation partial current density for Ag nanoparticles, VA-MoS_2, and VA-$Mo_{0.95}Nb_{0.05}S_2$. Reproduced with permission from ref [67]. Copyright 2017 ACS nano.

For the TM atoms as dopants in MoS_2, the introduction of V, Zr, and Hf into MoS_2 can significantly promote the desorption of CO from the MoS_2 edge, and thus achieving the optimal performance for electrocatalytic CO_2 reduction, because the TM doping can significantly modulate the binding energies of the CO_2 reduction species. For example, Mao et al. screened out three dopants (i.e., V, Zr, and Hf) with outstanding electrochemical performance (Figure 7a) [62]. The dopants can not only activate the O-C-O bond by enhancing the binding energy of CO_2, but also allow CO to

Preprints (www.preprints.org) | NOT PEER-REVIEWED | Posted: 29 August 2023 doi:10.20944/preprints202308.1932.v1

desorb more easily by reducing the binding energies of CO. Compared with pristine 2D MoS_2, the binding energies of CO are significantly decreased by 0.59, 0.59 and 0.58 eV for V-, Zr-and Hf-doped MoS_2 edges, respectively. In addition, the dopants position is extremely important to the catalytic activity for CO_2RR, but relatively the doping concentration is insignificant. Such conclusion has been early proved via the research work of Nørskov et al under DFT calculations about the electrocatalytic CO_2 reduction on MoS_2 edge with Mo edge replaced by TM atoms. As shown in Figure 7b, the closer the doping position is located to the active sites of the Mo edge, the more obvious the doping effect is, because single-atom metals can affect the local electronic structures of 2D MoS_2. This work developed an effective method to improve the electrocatalytic activity of 2D MoS_2 by doping near the active molybdenum at low doping concentrations. In addition, other studies about single-atom metal modified 2D MoS_2 (as shown in Table 1) also prove the importance of the intermediate *HCOO in the reaction pathway and potential determining steps.

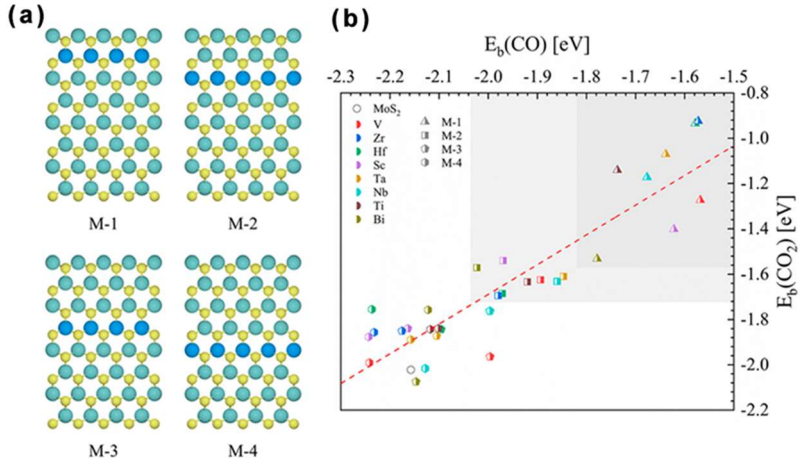

Figure 7. (**a**) TM-doped MoS_2 structures with different positions of dopants. The green, bule, and yellow balls represent Mo, TM, and S atoms, respectively. (**b**) Binding energies of CO_2 vs CO for the M-*x* (*x* = 1, 2, 3, 4) MoS_2. The *x* indicates the row next to the Mo edge for TM doping. Reproduced with permission from ref [62]. Copyright 2020 The Journal of Physical Chemistry C.

4. Single-atom Metal/2D MoS_2 Hybrid Nanomaterials for Water Splitting

4.1. Noble Metal Modified 2D MoS_2

In a conventional water electrolyzer, HER reaction occurs at the cathode, and H_2 is separated out, while OER reaction occurs at the anode, and O_2 is separated out (Figure 8a) [73-75]. Under standard conditions, a thermodynamic potential of 1.23 V is required to drive electrochemical water splitting (Figure 8b) for HER and OER. However, in real conditions, the input potential of water splitting in practical electrolyzers is much larger than 1.23 V. In general, high-performance electrocatalyst for water splitting is still focused on noble metal-based catalysts (e.g., Pt for HER and IrO_2 or RuO_2 for OER); however, it is necessary to develop noble metal-free electrocatalysts or decrease the loading amount of noble metals electrocatalysts because of the prohibitive cost and scarce reserve.

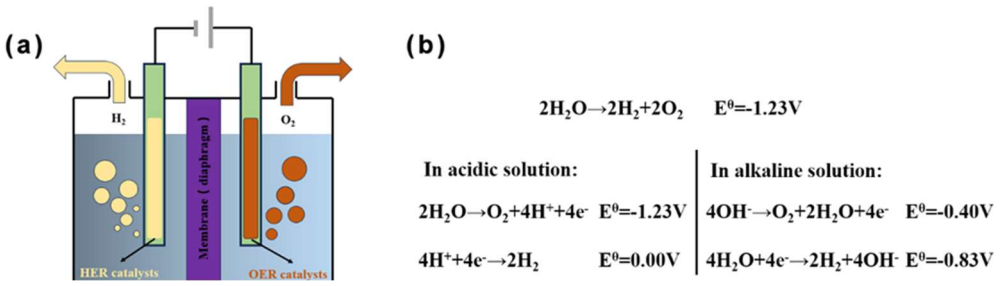

Preprints (www.preprints.org) | NOT PEER-REVIEWED | Posted: 29 August 2023 doi:10.20944/preprints202308.1932.v1

Figure 8. (**a**) Illustration of conventional water electrolyzers. (**b**) Water splitting reactions under acidic and alkaline conditions.

Single-atom noble metal catalysts (SACs) can not only decrease the loading amount, but also significantly improve the number of catalytic active sites via reducing the size of materials to the atomic-scale range, which can fully take advantage of reaction sites in electrocatalysts. For the hybrid system of single-atom noble metal modified 2D MoS_2, the noble metal doping can enhance the adsorption capacity of 2D MoS_2 for gas molecule and metal ions [76]. The introduced noble metals can not only function as active centers for facilitating water adsorption and dissociation, but also improve the electrical conductivity via modifying the electronic structure of 2D MoS_2 [77]. In addition, noble metal single atoms are able to change the chemical bond between H and S/Mo atoms, which can enhance the intrinsic activity of each active center for electrocatalytic water splitting [78]. The in-plane S position adjacent to the doped noble atoms can produce new active sites for HER [79]. At present, Pt@2D MoS_2 is still a hot spot in the field of single noble metal atoms/2D MoS_2 hybrid nanomaterials for electrocatalytic water splitting, and this catalyst is usually prepared by the one-pot method, which is beneficial to the uniform distribution of Pt atoms in the 2D MoS_2 plane. Pt doping can significantly reduce the activation energy of electrocatalytic water splitting. In addition to Pt atoms, noble metal atoms such as Ru, Pd and Au are also applied to enhance the electrocatalytic water splitting performance of 2D MoS_2. For example, the synergistic effect between S vacancies and Ru sites can improve the catalytic performance of active sites [80]. Doping Pd atoms can introduce abundant S vacancies and convert 2H MoS_2 into stable 1T-MoS_2, enhancing the electrical transport [81]. In addition, doping with Au atoms can modify the band structure of the 2D MoS_2, which is beneficial for the electronic transfer [82]. All the improvements in electrocatalytic performance indicate that doping noble metal atoms can improve the electrocatalytic water splitting performance of 2D MoS_2.

Compared with H_2 evolution, the release of diatomic O_2 is challenging because there are four electrons and four protons involved in the eventual formation of an O–O bond. In general, the elementary substances of Cu and Co are used for either HER or OER, but rarely for electrochemically overall water splitting. Xu et al. screened 28 metal single atoms supported on MoS_2 edges as bifunctional electrocatalysts for overall water splitting by using DFT calculations [78]. Authors proposed a simple equation including the chemical environment and local structure of the active center, which can be used as a new structure descriptor to forecast the oxygen evolution reaction activities for MoS_2-based SACs. Among these metal single atoms, the T1-vacancy (in which 37.5% of sulfur atoms are added to the initial Mo termination) modified using a Pt single atom exhibits the lowest theoretical overpotential for HER and OER, which is comparable to those of the noble-metal-group benchmark catalysts for overall water splitting, which. Compared with pure MoS_2 terminations, the Pt single atom can increase the intrinsic activity of each active center by changing the chemical bond between H and S/Mo atoms. The high OER performance is attributed to the moderate d band center of the single metal atom. By analyzing the electrical structure of S/Mo near the hydrogen, the improvement of intrinsic HER activity is attributed to the change of the bond between H and S/Mo.

Similarly, Bao et al. [15] and Zhang et al. [82] also reported that the electrocatalytic activity of Pt@MoS_2 in the HER process was greatly improved compared with pure MoS_2. With $(NH_4)_6Mo_7O_{24}$, H_2PtCl_6 and CS_2 as precursors, Pt@2D MoS_2 was synthesized through a one-pot chemical method, which realized the uniform distribution of Pt atoms in the 2D MoS_2 nanosheets. The transmission electron microscopy (TEM) image (Figure 9a) shows that the structure of Pt@2D MoS_2 is flower-like 2D nanosheets. As shown in Figure 9b, single Pt atoms uniformly disperse on the entire 2D nanosheets and substitute the Mo atoms. Compared with blank glassy carbon (GC) electrode and bulk MoS_2, the electrocatalytic activity of Pt@2D MoS_2 for HER is significantly improved after the Pt atom doping (Figure 9c). As shown in Tafel plots, different from Pt/C electrocatalyst (32 mV dec^{-1}), the value of Pt@MoS_2 (96 mV dec^{-1}) is closer to that of pure few-layer MoS_2 nanosheets (FL-MoS_2) (98 mV dec^{-1}), which indicates that the S atoms instead of the Pt atoms are the active sites of HER reaction (Figure 9d). Moreover, Pt@2D MoS_2 electrocatalysts exhibit show extremely stable performance

Preprints (www.preprints.org) | NOT PEER-REVIEWED | Posted: 29 August 2023 doi:10.20944/preprints202308.1932.v1

(Figure 9e and Figure 9f) because the current intensity and the potential values are nearly unchanged even after suffering from long-term cyclic voltammetric (CV) sweeps (>1000 CVs). All these enhancements are attributed to the activation of the in-plane S position adjacent to the doped Pt atom and the change of H adsorption free energy (ΔG_H) based on the DFT calculations, because Pt doping leads to the decrease of band gap, the improved the electron transport properties, and the reduced activation energy of water splitting.

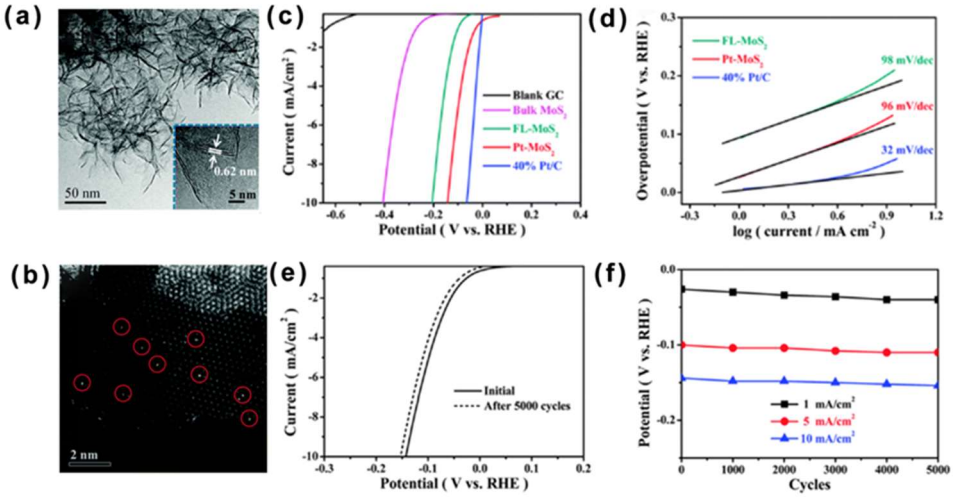

Figure 9. (**a**) TEM image and (**b**) HAADF-STEM images of Pt-MoS_2. (**c**) HER polarization curves for Pt–MoS_2 in comparison with blank GC electrode, bulk MoS_2, FL-MoS_2, and 40% Pt/C. (**d**) Tafel plots for FL-MoS_2, Pt–MoS_2, and 40% Pt/C, respectively. (**e**) Durability measurement of Pt–MoS_2. (**f**) Potential values recorded initially and after every 1000 CVs from the polarization curves of durability measurements for Pt–MoS_2 at 1 mA cm^{-2}, 5 mA cm^{-2} and 10 mA cm^{-2}, respectively. Reproduced with permission from ref [15]. Copyright 2015 The Royal Society of Chemistry.

4.2. Non-noble Metal Modified 2D MoS_2

Although anchoring single-atom noble metal onto 2D MoS_2 can enhance the electrocatalytic activity for overall water splitting, developing non-precious metals with comparable electrocatalysis activity with that of noble metal is still the best strategy for saving costs [83]. Transition-metal doping can not only modify the electronic structure of 2D MoS_2, but also induce lattice distortion and effectively increase the exchange current density, which can enlarge the surface active areas and improve the electrical conductivity [37,84,85]. 2D MoS_2 nanosheets exhibit excellent electrocatalytic performance for hydrogen evolution, especially the 2D MoS_2 with 1T-metallic phase with superior HER catalytic activity to 2H semiconducting phase. Therefore, coupling of MoS_2 with TM atoms with excellent OER activities can realize the improvement the overall water splitting performance [86,87].

Wang et al. developed a direct one-pot hydrothermal method to synthesize pure 1T-MoS_2 with flower-like morphology and high stability at a low temperature of 200 °C, and TMs (Ni, Co, Fe) were further doped by one-pot method to improve the HER activity and OER activity of 1T-MoS_2 in alkaline media [50]. As shown in Figure 10a, Gibbs free energy changes in the electrocatalytic reaction due to single-atom metals doping. This is because doping Fe, Co, and Ni atoms can change the electronic structure of MoS_2, which can decrease its adsorption of H_2O and increase the possibility of H_2O dissociation. In addition, consistent with XPS results, the charge difference density of Ni@1T-MoS_2 indicates that Ni plays a role in losing electrons and Mo acquires electrons (Figure 10b). In addition, Mo 3d spectrum exhibits a significant increase in electron density. Moreover, Ni@2D MoS_2 has the highest charge density at the Fermi surface (Figure 10c), which can accelerate electron exchange. In Figure 10d, DFT-optimized geometries of alkaline HER on Ni@1T-MoS_2 are exhibited, which shows the mechanism and intermediate steps of alkaline HER reaction for Ni@1T-MoS_2. Furthermore, as the molar ratio of Mo/Ni reaches ~6.7, the hybrid electrocatalyst can achieve the best electrocatalytic performance of η_{10} of 112 mV for HER and 224 mV for OER. The overall water

Preprints (www.preprints.org) | NOT PEER-REVIEWED | Posted: 29 August 2023 doi:10.20944/preprints202308.1932.v1

splitting reactivity is attributed to single atomic Ni that changes the electronic structure of 2D 1T-MoS_2.

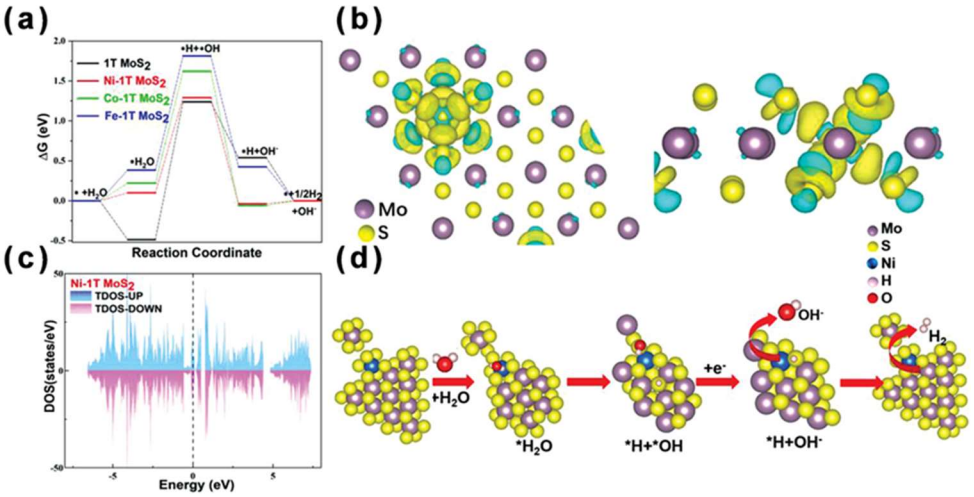

Figure 10. (**a**) Gibbs free energy diagrams for the H_2 production pathway on the 1T-MoS_2 and TM-doped 1T-MoS_2. (**b**) Charge difference density of Ni@1T-MoS_2. (**c**) DOS of Ni@1T-MoS_2. (**d**) DFT-optimized geometries of alkaline HER on Ni@1T-MoS_2. Reproduced with permission from ref [50]. Copyright 2020 Small.

Similarly, Zheng et al. prepared several selenium-doped MoS_2 nanofoam (Se-MoS_2-NF) with different Se content based on a one-pot solvothermal method [88]. Se-doped MoS_2 nanofoam has abundant spherical cavities (Figure 11a), which is beneficial for the mass transportation of reactants and increasing the number of active sites. Figure 11b shows the homogeneous distribution of Mo, S, and Se elements in Se-doped MoS_2 nanofoam. In addition, Se-MoS_2-NF has richer edges than both MoS_2 nanofoam (MoS_2-NF) and few-layer MoS_2 (MoS_2-FL) (Figure 11c), which means that the electrocatalytic HER performance of Se-MoS_2-NF can be significantly improved. HER polarization curves show that Se-MoS_2-NF exhibits much better HER activity than those of bulk MoS_2, MoS_2-FL, and MoS_2-NF (Figure 11d). Moreover, 9.1% is the best doping content of Se atom, and HER activity is the highest at this time (Figure 11e).

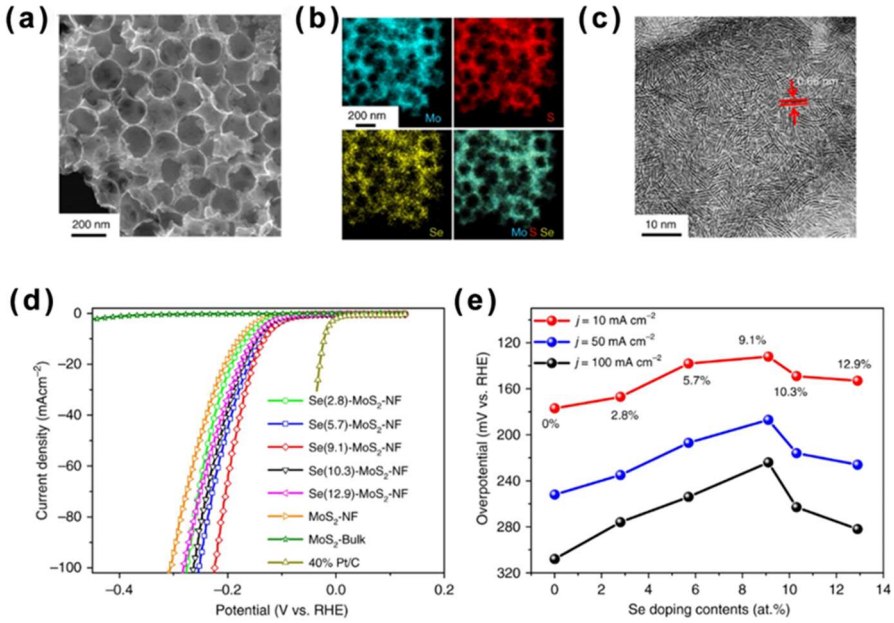

Figure 11. (**a**) SEM image, (**b**) EDX mappings, and (**c**) HRTEM image of the Se-MoS_2-NF. (**d**) HER polarization curves for the Se-MoS_2-NF with different Se deposited contents. (**e**) Changes of

Preprints (www.preprints.org) | NOT PEER-REVIEWED | Posted: 29 August 2023 doi:10.20944/preprints202308.1932.v1

overpotentials depending on the Se deposited content at different current densities. Reproduced with permission from ref [88]. Copyright 2020 Nature communications.

Qiao et al. proposed a simple, inexpensive way for modifying MoS_2 nanosheets on Cu nanorods to design MoS_2/Cu structure as a multifunctional catalyst [72]. The electrocatalyst shows markedly improved performances for both HER and OER and great durability in alkaline media. The facial and scalable synthetic effect between Cu nanorods and MoS_2 nanosheets leads to great electrocatalytic performance. This study provides the possible strategy to develop electrocatalysts with desired catalytic performance and stability through simple and large-scale manufacturing techniques. Similarly, Zhu et al. explored the electrocatalytic water splitting activity of Cu@2H-MoS_2 and Co@2H-MoS_2 by DFT calculations [89]. It is found that anchoring single-atom Cu or Co onto 2D 2H-MoS_2 can change the surface charge distribution and electronic band structure of 2H-MoS_2. By doping single-atom Cu or Co, inert in-plane S-atoms of 2D 2H-MoS_2 can be activated, thus significantly improving the electrochemical activity of overall water splitting. Relatively, Co@2H-MoS_2 shows better HER performance with smaller Gibbs free energy of the hydrogen adsorption ($\Delta G_H = 0.08$ eV), and Cu@2H-MoS_2 exhibits lower energy barrier and a reduced overpotential of 1.25 eV for OER.

Qi et al. explored a top-down assembly/leaching method to realize Co array covalently anchored onto distorted 1T-MoS_2 nanosheets (SA Co-D 1T-MoS_2) [52]. As shown in Figure 12a-d, the atomic dispersion of Co atoms and the phase transformation of MoS_2 are observed. Specifically, both the HAADF-STEM image (Figure 12b) and simulated pattern (Figure 12c, d) demonstrate the obvious interface between SA Co-D 1T-MoS_2 and 2H MoS_2. Single Co atoms are homogeneously distributed on the top of Mo atoms on the MoS_2 slab. The SA Co-D 1T-MoS_2 electrocatalyst containing 3.54% Co (wt.%) shows an incredibly small onset overpotential for HER, even comparable with that of 10% Pt/C (Figure 12e). In addition, the Tafel slope of SA Co-D 1T-MoS_2 (32 mV dec^{-1}) is also comparable to that of Pt/C (30 mV dec^{-1}), preceding those of non-Pt based electrocatalysts (Figure 12f). Moreover, the low Tafel slope exhibits that a Tafel rate-determining-step mechanism, rather than the common Volmer reaction, is responsible for electrocatalytic HER of SA Co-D 1T-MoS_2 [90].

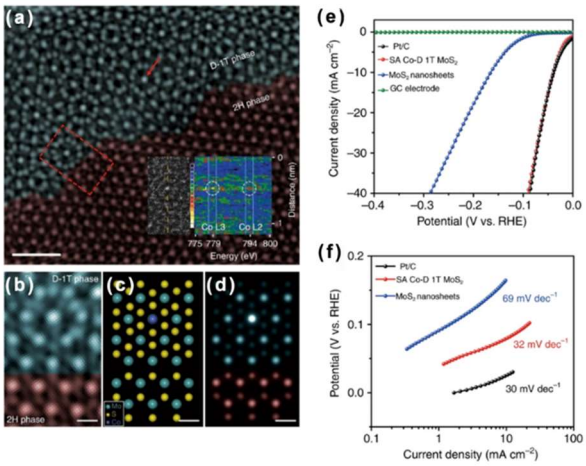

Figure 12. (**a**) Aberration-corrected HAADF-STEM image of SA Co-D 1T-MoS_2. (**b**) Enlarged HAADF-STEM image in the red square area of Figure 12**a**. (**c**) Theoretical model and (**d**) simulated STEM images. (**e**) Polarization curves and (**f**) Tafel plots of different catalysts. Reproduced with permission from ref [52]. Copyright 2019 Nature communications.

Table 2. Summary of typical single-atom metal/2D MoS_2 hybrid nanomaterials for water splitting.

Catalyst	Electrolyte	η (mV)/best ratio (w.t.% or concentration)	Tafel slope (mV dec^{-1})	Stability test	Ref

Preprints (www.preprints.org) | NOT PEER-REVIEWED | Posted: 29 August 2023 doi:10.20944/preprints202308.1932.v1

Co/2D MoS_2	0.5 M H_2SO_4	42/3.5% Co/1T-MoS_2	32	10,000 CVs	[52]
Pt/2D MoS_2	0.1 M H_2SO_4	60/1.5% Pt /MoS_2	96	5000 CVs	[15]
Pd/2D MoS_2	0.5 M H_2SO_4	89/1% Pd/1T-MoS_2	62	5000 CVs	[81]
Ni/2D MoS_2	0.5 M H_2SO_4	98/Ni/MoS_2	103	2000 CVs	[91]
Ru/2D MoS_2	0.5 M H_2SO_4	114/46 μg cm^{-2} Ru/MoS_2	-	10 h	[92]
Cu/2D MoS_2	0.5 M H_2SO_4	131/1% Cu/MoS_2	51	7 h	[49]
Fe, Co, Ni, Pd, Pt/2D MoS_2	0.5 M H_2SO_4	140/2.7% Pd/1T-MoS_2	57	1000 CVs	[93]
Ni/2D MoS_2	0.5 M H_2SO_4	174/1% Ni/MoS_2	69	1000 CVs	[94]
Au, Pt, Pd/2D MoS_2	0.5 M H_2SO_4	210/1.1% Pt/MoS_2	104	5 h	[58]
Ni/2D MoS_2	0.5 M H_2SO_4	263/2.7% Ni/MoS_2	81	1000 CVs	[95]
Ru/2D MoS_2	1.0 M PBS	125/46 μg cm^{-2} Ru/ MoS_2	-	10 h	[92]
Ru/2D MoS_2	1.0 M KOH	41/46 μg cm^{-2} Ru/ MoS_2	114	20 h	[92]
Ir/2D MoS_2	1.0 M KOH	44/Ir/1T-MoS_2	32	9000 CVs	[96]
Ni/2D MoS_2	1.0 M KOH	110/Ni/MoS_2	119	2000 CVs	[91]

Note: overpotential value (η) and stability test were performed at the current density of 10 mA cm^{-2}; CVs, cycles.

5. Challenges and Prospects

In this review, main advantages and features, synthesis methods, and applications of single-atom metal/2D-MoS_2 hybrid nanomaterials for electrocatalytic CO_2RR and water splitting were comprehensively discussed. Our discussions highlighted strategies, typical examples, and possible mechanism of improving electrocatalytic activity. Although research has considerably progressed in single-atom metal/2D-MoS_2 hybrid for CO_2RR and water splitting [59,97-100], certain challenges remain in the development of for fabricating low-cost and high-performance electrocatalysts, solving the aggregation of single-atom catalysts as number of active sites and loading amounts increasing [101,102], and clarifying the reaction mechanism [103-105].

Therefore, from a long-term view, more efforts in the future are focused on control synthesis, structure-property characterization, and reaction mechanism. First, it is necessary to work hard on controllable preparation to ensure the dispersion of single metal atoms and the catalytic activity of hybrid catalysts [106], because the control, high-quality, and large-scale synthesis of single-atom catalysts is the precondition or bottleneck for deeply understanding structure-property relationship and reaction mechanism. For example, the non-noble metals of SACs such as Fe, Ni, and Cu nanoparticles are easily oxidized in air [12]. Second, the research efforts in future may be focused on the development and utilization of some in-situ characterization methods (e.g., in situ Fourier transform infrared spectroscopy) and theoretical predictions (e.g., DFT or machine learning) for better understanding of structure-property relationship [107-111], especially the relationship between the defects of these hybrid nanomaterials and their electrocatalytic activity. The DFT calculation can simulate the electrocatalytic reaction efficiency of single-atom metal/ 2D MoS_2 hybrid nanomaterials and clarify the electron transfer mechanism between 2D MoS_2 and single metal atoms [12]. Last but not least, expect for the electrocatalyst itself, to accurately identify the clear catalytic mechanisms, the fundamental research and optimized standard experimental systems of electrocatalytic water splitting and CO_2RR are still required [9].

Author Contributions: Conceptualization, X. G. (Xiaorong Gan); writing—original draft preparation, J. W. (Jiaohao Wang); writing—review and editing, X. G. (Xiaorong Gan), T. Z. (Tianhao Zhu), D. Z. (Dan Zhao), Y. A. (Yanhui Ao), P. Z. (Peifang Wang); All authors have read and agreed to the published version of the manuscript.

Funding: This work was supported by the National Natural Science Foundation of China (No. 52000059). Also, this study was funded by the Key Lab of Modern Optical Technologies of Jiangsu Province, Soochow University.

References

1. Chen, Y.; Ji, S.; Chen, C.; Peng, Q.; Wang, D.; Li, Y. Single-atom catalysts: synthetic strategies and electrochemical applications. Joule 2018, 2, 1242-1264.
2. Zhang, J.; Zhao, Y.; Guo, X.; Chen, C.; Dong, C.-L.; Liu, R.-S.; Han, C.-P.; Li, Y.; Gogotsi, Y.; Wang, G. Single platinum atoms immobilized on an MXene as an efficient catalyst for the hydrogen evolution reaction. Nature Catalysis 2018, 1, 985-992.
3. Gu, J.; Hsu, C.-S.; Bai, L.; Chen, H.M.; Hu, X. Atomically dispersed Fe^{3+} sites catalyze efficient CO_2 electroreduction to CO. Science 2019, 364, 1091-1094.
4. Wang, A.; Li, J.; Zhang, T. Heterogeneous single-atom catalysis. Nature Reviews Chemistry 2018, 2, 65-81.
5. Xu, J.; Lai, S.; Qi, D.; Hu, M.; Peng, X.; Liu, Y.; Liu, W.; Hu, G.; Xu, H.; Li, F. Atomic Fe-Zn dual-metal sites for high-efficiency pH-universal oxygen reduction catalysis. Nano Research 2021, 14, 1374-1381.
6. Zhang, N.; Zhang, X.; Tao, L.; Jiang, P.; Ye, C.; Lin, R.; Huang, Z.; Li, A.; Pang, D.; Yan, H. Silver single-atom catalyst for efficient electrochemical CO_2 reduction synthesized from thermal transformation and surface reconstruction. Angewandte Chemie International Edition 2021, 60, 6170-6176.
7. Gan, X.; Lei, D.; Ye, R.; Zhao, H.; Wong, K.-Y. Transition metal dichalcogenide-based mixed-dimensional heterostructures for visible-light-driven photocatalysis: Dimensionality and interface engineering. Nano Research 2021, 14, 2003-2022.
8. Qiao, B.; Wang, A.; Yang, X.; Allard, L.F.; Jiang, Z.; Cui, Y.; Liu, J.; Li, J.; Zhang, T. Single-atom catalysis of CO oxidation using Pt_1/FeO_x. Nature chemistry 2011, 3, 634-641.
9. Yang, X.-F.; Wang, A.; Qiao, B.; Li, J.; Liu, J.; Zhang, T. Single-atom catalysts: a new frontier in heterogeneous catalysis. Accounts of chemical research 2013, 46, 1740-1748.

10. Jones, J.; Xiong, H.; DeLaRiva, A.T.; Peterson, E.J.; Pham, H.; Challa, S.R.; Qi, G.; Oh, S.; Wiebenga, M.H.; Pereira Hernández, X.I. Thermally stable single-atom platinum-on-ceria catalysts via atom trapping. Science 2016, 353, 150-154.
11. Sun, J.-F.; Wu, J.-T.; Xu, Q.-Q.; Zhou, D.; Yin, J.-Z. CO_2 electrochemical reduction using single-atom catalysts. Preparation, characterization and anchoring strategies: a review. Environmental Chemistry Letters 2020, 18, 1593-1623.
12. Kwon, K.C.; Suh, J.M.; Varma, R.S.; Shokouhimehr, M.; Jang, H.W. Electrocatalytic water splitting and CO_2 reduction: sustainable solutions via single-atom catalysts supported on 2D materials. Small Methods 2019, 3, 1800492.
13. Lee, W.H.; Ko, Y.-J.; Kim, J.-Y.; Min, B.K.; Hwang, Y.J.; Oh, H.-S. Single-atom catalysts for the oxygen evolution reaction: recent developments and future perspectives. Chemical Communications 2020, 56, 12687-12697.
14. Li, X.; Cui, P.; Zhong, W.; Li, J.; Wang, X.; Wang, Z.; Jiang, J. Graphitic carbon nitride supported single-atom catalysts for efficient oxygen evolution reaction. Chemical Communications 2016, 52, 13233-13236.
15. Deng, J.; Li, H.; Xiao, J.; Tu, Y.; Deng, D.; Yang, H.; Tian, H.; Li, J.; Ren, P.; Bao, X. Triggering the electrocatalytic hydrogen evolution activity of the inert two-dimensional MoS_2 surface via single-atom metal doping. Energy & environmental science 2015, 8, 1594-1601.
16. He, T.; Zhang, C.; Du, A. Single-atom supported on graphene grain boundary as an efficient electrocatalyst for hydrogen evolution reaction. Chemical Engineering Science 2019, 194, 58-63.
17. Vancsó, P.; Popov, Z.I.; Peto˝, J.n.; Ollár, T.; Dobrik, G.; Pap, J.z.S.; Hwang, C.; Sorokin, P.B.; Tapasztó, L. Transition metal chalcogenide single layers as an active platform for single-atom catalysis. ACS Energy Letters 2019, 4, 1947-1953.
18. Zhou, X.; Li, K.; Lin, Y.; Song, L.; Liu, J.; Liu, Y.; Zhang, L.; Wu, Z.; Song, S.; Li, J. A single-atom manipulation approach for synthesis of atomically mixed nanoalloys as efficient catalysts. Angewandte Chemie 2020, 132, 13670-13676.
19. Su, H.; Zhou, W.; Zhang, H.; Zhou, W.; Zhao, X.; Li, Y.; Liu, M.; Cheng, W.; Liu, Q. Dynamic evolution of solid–liquid electrochemical interfaces over single-atom active sites. Journal of the American Chemical Society 2020, 142, 12306-12313.
20. Zhang, X.; Guo, J.; Guan, P.; Liu, C.; Huang, H.; Xue, F.; Dong, X.; Pennycook, S.J.; Chisholm, M.F. Catalytically active single-atom niobium in graphitic layers. Nature communications 2013, 4, 1924.
21. Gan, X.; Zhang, J.; Liu, J.; Bai, Y.; Su, X.; Wang, W.; Cao, Z.; Zhao, H.; Ao, Y.; Wang, P. Polyaniline Functionalization of Defective 1T-MoS_2 Nanosheets for Improved Electron and Mass Transfer: Implications for Electrochemical Sensors. ACS Applied Nano Materials 2023.
22. Hou, C.C.; Zou, L.; Sun, L.; Zhang, K.; Liu, Z.; Li, Y.; Li, C.; Zou, R.; Yu, J.; Xu, Q. Single-atom iron catalysts on overhang-eave carbon cages for high-performance oxygen reduction reaction. Angewandte Chemie 2020, 132, 7454-7459.
23. Zhu, J.; Cai, L.; Yin, X.; Wang, Z.; Zhang, L.; Ma, H.; Ke, Y.; Du, Y.; Xi, S.; Wee, A.T. Enhanced electrocatalytic hydrogen evolution activity in single-atom Pt-decorated VS_2 nanosheets. ACS nano 2020, 14, 5600-5608.
24. Rao, R.G.; Blume, R.; Hansen, T.W.; Fuentes, E.; Dreyer, K.; Moldovan, S.; Ersen, O.; Hibbitts, D.D.; Chabal, Y.J.; Schlögl, R. Interfacial charge distributions in carbon-supported palladium catalysts. Nature communications 2017, 8, 340.
25. Gan, X.; Zhao, H.; Quan, X. Two-dimensional MoS_2: A promising building block for biosensors. Biosensors and Bioelectronics 2017, 89, 56-71.
26. Liu, T.; Zhao, X.; Liu, X.; Xiao, W.; Luo, Z.; Wang, W.; Zhang, Y.; Liu, J.-C. Understanding the hydrogen evolution reaction activity of doped single-atom catalysts on two-dimensional $GaPS_4$ by DFT and machine learning. Journal of Energy Chemistry 2023, 81, 93-100.
27. Xiao, Z.; Gan, X.; Zhu, T.; Lei, D.; Zhao, H.; Wang, P. Activating the Basal Planes in 2H-$MoTe_2$ Monolayers by Incorporating Single-Atom Dispersed N or P for Enhanced Electrocatalytic Overall Water Splitting. Advanced Sustainable Systems 2022, 6, 2100515.
28. Gan, X.; Lei, D.; Wong, K.-Y. Two-dimensional layered nanomaterials for visible-light-driven photocatalytic water splitting. Materials today energy 2018, 10, 352-367.
29. Pan, U.N.; Paudel, D.R.; Das, A.K.; Singh, T.I.; Kim, N.H.; Lee, J.H. Ni-nanoclusters hybridized 1T–Mn–VTe_2 mesoporous nanosheets for ultra-low potential water splitting. Applied Catalysis B: Environmental 2022, 301, 120780.
30. Ertl, G.; Knözinger, H.; Weitkamp, J. Handbook of heterogeneous catalysis; VCH Weinheim: 1997; Volume 2.
31. Yang, J.; Mohmad, A.R.; Wang, Y.; Fullon, R.; Song, X.; Zhao, F.; Bozkurt, I.; Augustin, M.; Santos, E.J.; Shin, H.S. Ultrahigh-current-density niobium disulfide catalysts for hydrogen evolution. Nature materials 2019, 18, 1309-1314.

32. Gusmão, R.; Veselý, M.; Sofer, Z.k. Recent developments on the single atom supported at 2D materials beyond graphene as catalysts. Acs Catalysis 2020, 10, 9634-9648.
33. Shi, Y.; Zhou, Y.; Yang, D.-R.; Xu, W.-X.; Wang, C.; Wang, F.-B.; Xu, J.-J.; Xia, X.-H.; Chen, H.-Y. Energy level engineering of MoS_2 by transition-metal doping for accelerating hydrogen evolution reaction. Journal of the American Chemical Society 2017, 139, 15479-15485.
34. Asadi, M.; Kim, K.; Liu, C.; Addepalli, A.V.; Abbasi, P.; Yasaei, P.; Phillips, P.; Behranginia, A.; Cerrato, J.M.; Haasch, R. Nanostructured transition metal dichalcogenide electrocatalysts for CO_2 reduction in ionic liquid. Science 2016, 353, 467-470.
35. Gan, X.; Lee, L.Y.S.; Wong, K.-y.; Lo, T.W.; Ho, K.H.; Lei, D.Y.; Zhao, H. 2H/1T phase transition of multilayer MoS_2 by electrochemical incorporation of S vacancies. ACS Applied Energy Materials 2018, 1, 4754-4765.
36. Gan, X.; Zhao, H.; Lei, D.; Wang, P. Improving electrocatalytic activity of 2H-MoS_2 nanosheets obtained by liquid phase exfoliation: Covalent surface modification versus interlayer interaction. Journal of Catalysis 2020, 391, 424-434.
37. Zhang, J.; Wang, T.; Pohl, D.; Rellinghaus, B.; Dong, R.; Liu, S.; Zhuang, X.; Feng, X. Interface engineering of MoS_2/Ni_3S_2 heterostructures for highly enhanced electrochemical overall-water-splitting activity. Angewandte Chemie 2016, 128, 6814-6819.
38. Linghu, Y.; Tong, T.; Li, C.; Wu, C. The catalytic mechanism of CO_2 electrochemical reduction over transition metal-modified 1T'-MoS_2 monolayers. Applied Surface Science 2022, 590, 153001.
39. Ji, S.; Chen, Y.; Wang, X.; Zhang, Z.; Wang, D.; Li, Y. Chemical synthesis of single atomic site catalysts. Chemical Reviews 2020, 120, 11900-11955.
40. Cheng, N.; Stambula, S.; Wang, D.; Banis, M.N.; Liu, J.; Riese, A.; Xiao, B.; Li, R.; Sham, T.-K.; Liu, L.-M. Platinum single-atom and cluster catalysis of the hydrogen evolution reaction. Nature communications 2016, 7, 13638.
41. Lu, Y.; Kuo, C.-T.; Kovarik, L.; Hoffman, A.S.; Boubnov, A.; Driscoll, D.M.; Morris, J.R.; Bare, S.R.; Karim, A.M. A versatile approach for quantification of surface site fractions using reaction kinetics: The case of CO oxidation on supported Ir single atoms and nanoparticles. Journal of Catalysis 2019, 378, 121-130.
42. Repp, J.; Moresco, F.; Meyer, G.; Rieder, K.-H.; Hyldgaard, P.; Persson, M. Substrate mediated long-range oscillatory interaction between adatoms: Cu/Cu(111). Physical Review Letters 2000, 85, 2981.
43. Ji, Q.; Zhang, Y.; Zhang, Y.; Liu, Z. Chemical vapour deposition of group-VIB metal dichalcogenide monolayers: engineered substrates from amorphous to single crystalline. Chemical Society Reviews 2015, 44, 2587-2602.
44. Xiong, Q.; Zhang, X.; Wang, H.; Liu, G.; Wang, G.; Zhang, H.; Zhao, H. One-step synthesis of cobalt-doped MoS_2 nanosheets as bifunctional electrocatalysts for overall water splitting under both acidic and alkaline conditions. Chemical Communications 2018, 54, 3859-3862.
45. Zhang, F.; Momeni, K.; AlSaud, M.A.; Azizi, A.; Hainey, M.F.; Redwing, J.M.; Chen, L.-Q.; Alem, N. Controlled synthesis of 2D transition metal dichalcogenides: from vertical to planar MoS_2. 2D Materials 2017, 4, 025029.
46. Zhang, H. Ultrathin two-dimensional nanomaterials. ACS nano 2015, 9, 9451-9469.
47. Li, J.; Chen, S.; Quan, F.; Zhan, G.; Jia, F.; Ai, Z.; Zhang, L. Accelerated dinitrogen electroreduction to ammonia via interfacial polarization triggered by single-atom protrusions. Chem 2020, 6, 885-901.
48. Zeng, Z.; Yin, Z.; Huang, X.; Li, H.; He, Q.; Lu, G.; Boey, F.; Zhang, H. Single-layer semiconducting nanosheets: high-yield preparation and device fabrication. Angewandte Chemie 2011, 123, 11289-11293.
49. Ji, L.; Yan, P.; Zhu, C.; Ma, C.; Wu, W.; Wei, C.; Shen, Y.; Chu, S.; Wang, J.; Du, Y. One-pot synthesis of porous 1T-phase MoS_2 integrated with single-atom Cu doping for enhancing electrocatalytic hydrogen evolution reaction. Applied Catalysis B: Environmental 2019, 251, 87-93.
50. Wang, G.; Zhang, G.; Ke, X.; Chen, X.; Chen, X.; Wang, Y.; Huang, G.; Dong, J.; Chu, S.; Sui, M. Direct Synthesis of Stable 1T-MoS_2 Doped with Ni Single Atoms for Water Splitting in Alkaline Media. Small 2022, 18, 2107238.
51. Wang, X.; Zhang, Y.; Wu, J.; Zhang, Z.; Liao, Q.; Kang, Z.; Zhang, Y. Single-atom engineering to ignite 2D transition metal dichalcogenide based catalysis: Fundamentals, progress, and beyond. Chemical Reviews 2021, 122, 1273-1348.
52. Qi, K.; Cui, X.; Gu, L.; Yu, S.; Fan, X.; Luo, M.; Xu, S.; Li, N.; Zheng, L.; Zhang, Q. Single-atom cobalt array bound to distorted 1T MoS_2 with ensemble effect for hydrogen evolution catalysis. Nature communications 2019, 10, 5231.
53. Huang, Y.; Sun, Y.; Zheng, X.; Aoki, T.; Pattengale, B.; Huang, J.; He, X.; Bian, W.; Younan, S.; Williams, N. Atomically engineering activation sites onto metallic 1T-MoS_2 catalysts for enhanced electrochemical hydrogen evolution. Nature communications 2019, 10, 982.
54. Wang, Y.; Han, P.; Lv, X.; Zhang, L.; Zheng, G. Defect and interface engineering for aqueous electrocatalytic CO_2 reduction. Joule 2018, 2, 2551-2582.

55. Deng, T.; Zheng, W.; Zhang, W. Increasing the range of non-noble-metal single-atom catalysts. Chinese Journal of Catalysis 2017, 38, 1489-1497.
56. Zhang, H.; Liu, G.; Shi, L.; Ye, J. Single-atom catalysts: emerging multifunctional materials in heterogeneous catalysis. Advanced Energy Materials 2018, 8, 1701343.
57. Thomas, J.M.; Saghi, Z.; Gai, P.L. Can a single atom serve as the active site in some heterogeneous catalysts? Topics in Catalysis 2011, 54, 588-594.
58. Xuan, N.; Chen, J.; Shi, J.; Yue, Y.; Zhuang, P.; Ba, K.; Sun, Y.; Shen, J.; Liu, Y.; Ge, B. Single-atom electroplating on two dimensional materials. Chemistry of Materials 2018, 31, 429-435.
59. Meng, Z.; Fan, J.; Chen, A.; Xie, X. Functionalized MoS_2 catalysts for CO_2 capture and conversion: a review. Materials Today Chemistry 2023, 29, 101449.
60. Detz, H.; Butera, V. Insights into the mechanistic CO_2 conversion to methanol on single Ru atom anchored on MoS_2 monolayer. Molecular Catalysis 2023, 535, 112878.
61. Ren, Y.; Sun, X.; Qi, K.; Zhao, Z. Single atom supported on MoS_2 as efficient electrocatalysts for the CO_2 reduction reaction: A DFT study. Applied Surface Science 2022, 602, 154211.
62. Mao, X.; Wang, L.; Xu, Y.; Li, Y. Modulating the MoS_2 edge structures by doping transition metals for electrocatalytic CO_2 reduction. The Journal of Physical Chemistry C 2020, 124, 10523-10529.
63. Liu, J.; Jiao, M.; Lu, L.; Barkholtz, H.M.; Li, Y.; Wang, Y.; Jiang, L.; Wu, Z.; Liu, D.-j.; Zhuang, L. High performance platinum single atom electrocatalyst for oxygen reduction reaction. Nature communications 2017, 8, 15938.
64. Zhao, Q.; Zhang, C.; Hu, R.; Du, Z.; Gu, J.; Cui, Y.; Chen, X.; Xu, W.; Cheng, Z.; Li, S. Selective etching quaternary MAX phase toward single atom copper immobilized MXene ($Ti_3C_2Cl_x$) for efficient CO_2 electroreduction to methanol. ACS nano 2021, 15, 4927-4936.
65. Gong, Y.-N.; Zhong, W.; Li, Y.; Qiu, Y.; Zheng, L.; Jiang, J.; Jiang, H.-L. Regulating photocatalysis by spin-state manipulation of cobalt in covalent organic frameworks. Journal of the American Chemical Society 2020, 142, 16723-16731.
66. Hong, X.; Chan, K.; Tsai, C.; Nørskov, J.K. How doped MoS_2 breaks transition-metal scaling relations for CO_2 electrochemical reduction. Acs Catalysis 2016, 6, 4428-4437.
67. Abbasi, P.; Asadi, M.; Liu, C.; Sharifi-Asl, S.; Sayahpour, B.; Behranginia, A.; Zapol, P.; Shahbazian-Yassar, R.; Curtiss, L.A.; Salehi-Khojin, A. Tailoring the edge structure of molybdenum disulfide toward electrocatalytic reduction of carbon dioxide. ACS nano 2017, 11, 453-460.
68. Yu, Q. Theoretical studies of non-noble metal single-atom catalyst Ni_1/MoS_2: Electronic structure and electrocatalytic CO_2 reduction. Science China Materials 2022, 1-10.
69. Nørskov, J.K.; Rossmeisl, J.; Logadottir, A.; Lindqvist, L.; Kitchin, J.R.; Bligaard, T.; Jonsson, H. Origin of the overpotential for oxygen reduction at a fuel-cell cathode. The Journal of Physical Chemistry B 2004, 108, 17886-17892.
70. Huang, W.; Zhou, D.; Yang, H.; Liu, X.; Luo, J. Dual-doping promotes the carbon dioxide electroreduction activity of MoS_2 nanosheet array. ACS Applied Energy Materials 2021, 4, 7492-7496.
71. Salehi-Khojin, A.; Jhong, H.-R.M.; Rosen, B.A.; Zhu, W.; Ma, S.; Kenis, P.J.; Masel, R.I. Nanoparticle silver catalysts that show enhanced activity for carbon dioxide electrolysis. The Journal of Physical Chemistry C 2013, 117, 1627-1632.
72. Ilyas, T.; Raziq, F.; Ali, S.; Zada, A.; Ilyas, N.; Shaha, R.; Wang, Y.; Qiao, L. Facile synthesis of MoS_2/Cu as trifunctional catalyst for electrochemical overall water splitting and photocatalytic CO_2 conversion. Materials & Design 2021, 204, 109674.
73. Wang, X.; Zheng, Y.; Sheng, W.; Xu, Z.J.; Jaroniec, M.; Qiao, S.-Z. Strategies for design of electrocatalysts for hydrogen evolution under alkaline conditions. Materials Today 2020, 36, 125-138.
74. Zhu, J.; Hu, L.; Zhao, P.; Lee, L.Y.S.; Wong, K.-Y. Recent advances in electrocatalytic hydrogen evolution using nanoparticles. Chemical reviews 2019, 120, 851-918.
75. Pham, V.P.; Yeom, G.Y. Recent advances in doping of molybdenum disulfide: industrial applications and future prospects. Advanced Materials 2016, 28, 9024-9059.
76. Zhao, Q.; Zhang, Z.; Ouyang, X. Adsorption of radionuclides on the monolayer MoS_2. Materials Research Express 2018, 5, 045506.
77. Tian, L.; Li, Z.; Xu, X.; Zhang, C. Advances in noble metal (Ru, Rh, and Ir) doping for boosting water splitting electrocatalysis. Journal of Materials Chemistry A 2021, 9, 13459-13470.
78. Xu, X.; Xu, H.; Cheng, D. Design of high-performance MoS_2 edge supported single-metal atom bifunctional catalysts for overall water splitting via a simple equation. Nanoscale 2019, 11, 20228-20237.
79. Zhang, X.; Zhou, F.; Zhang, S.; Liang, Y.; Wang, R. Engineering MoS_2 basal planes for hydrogen evolution via synergistic ruthenium doping and nanocarbon hybridization. Advanced Science 2019, 6, 1900090.
80. Jiang, K.; Luo, M.; Liu, Z.; Peng, M.; Chen, D.; Lu, Y.-R.; Chan, T.-S.; de Groot, F.M.; Tan, Y. Rational strain engineering of single-atom ruthenium on nanoporous MoS_2 for highly efficient hydrogen evolution. Nature Communications 2021, 12, 1687.

81. Luo, Z.; Ouyang, Y.; Zhang, H.; Xiao, M.; Ge, J.; Jiang, Z.; Wang, J.; Tang, D.; Cao, X.; Liu, C. Chemically activating MoS_2 via spontaneous atomic palladium interfacial doping towards efficient hydrogen evolution. Nature communications 2018, 9, 2120.
82. Zhang, Z.; Chen, K.; Zhao, Q.; Huang, M.; Ouyang, X. Electrocatalytic and photocatalytic performance of noble metal doped monolayer MoS_2 in the hydrogen evolution reaction: a first principles study. Nano Materials Science 2021, 3, 89-94.
83. Xue, Y.; Bai, X.; Xu, Y.; Yan, Q.; Zhu, M.; Zhu, K.; Ye, K.; Yan, J.; Cao, D.; Wang, G. Vertically oriented Ni-doped MoS_2 nanosheets supported on hollow carbon microtubes for enhanced hydrogen evolution reaction and water splitting. Composites Part B: Engineering 2021, 224, 109229.
84. Li, M.; Zhao, Z.; Xia, Z.; Yang, Y.; Luo, M.; Huang, Y.; Sun, Y.; Chao, Y.; Yang, W.; Yang, W. Lavender-like Ga-doped Pt_3Co nanowires for highly stable and active electrocatalysis. ACS Catalysis 2020, 10, 3018-3026.
85. Wang, C.; Xu, H.; Shang, H.; Jin, L.; Chen, C.; Wang, Y.; Yuan, M.; Du, Y. Ir-doped Pd nanosheet assemblies as bifunctional electrocatalysts for advanced hydrogen evolution reaction and liquid fuel electrocatalysis. Inorganic chemistry 2020, 59, 3321-3329.
86. Liu, J.; Wang, J.; Zhang, B.; Ruan, Y.; Wan, H.; Ji, X.; Xu, K.; Zha, D.; Miao, L.; Jiang, J. Mutually beneficial Co_3O_4@MoS_2 heterostructures as a highly efficient bifunctional catalyst for electrochemical overall water splitting. Journal of Materials Chemistry A 2018, 6, 2067-2072.
87. Muthurasu, A.; Maruthapandian, V.; Kim, H.Y. Metal-organic framework derived Co_3O_4/MoS_2 heterostructure for efficient bifunctional electrocatalysts for oxygen evolution reaction and hydrogen evolution reaction. Applied Catalysis B: Environmental 2019, 248, 202-210.
88. Zheng, Z.; Yu, L.; Gao, M.; Chen, X.; Zhou, W.; Ma, C.; Wu, L.; Zhu, J.; Meng, X.; Hu, J. Boosting hydrogen evolution on MoS_2 via co-confining selenium in surface and cobalt in inner layer. Nature communications 2020, 11, 3315.
89. Zhu, T.; Gan, X.; Xiao, Z.; Dai, S.; Xiao, H.; Zhang, S.; Dong, S.; Zhao, H.; Wang, P. Single-atom dispersed Cu or Co on 2H-MoS_2 monolayer for improving electrocatalytic activity of overall water splitting. Surfaces and Interfaces 2021, 27, 101538.
90. Liang, H.-W.; Brüller, S.; Dong, R.; Zhang, J.; Feng, X.; Müllen, K. Molecular metal–N_x centres in porous carbon for electrocatalytic hydrogen evolution. Nature communications 2015, 6, 7992.
91. Wang, Q.; Zhao, Z.L.; Dong, S.; He, D.; Lawrence, M.J.; Han, S.; Cai, C.; Xiang, S.; Rodriguez, P.; Xiang, B. Design of active nickel single-atom decorated MoS_2 as a pH-universal catalyst for hydrogen evolution reaction. Nano Energy 2018, 53, 458-467.
92. Wang, D.; Li, Q.; Han, C.; Xing, Z.; Yang, X. Single-atom ruthenium based catalyst for enhanced hydrogen evolution. Applied Catalysis B: Environmental 2019, 249, 91-97.
93. Lau, T.H.; Wu, S.; Kato, R.; Wu, T.-S.; Kulhavy, J.; Mo, J.; Zheng, J.; Foord, J.S.; Soo, Y.-L.; Suenaga, K. Engineering monolayer 1T-MoS_2 into a bifunctional electrocatalyst via sonochemical doping of isolated transition metal atoms. ACS Catalysis 2019, 9, 7527-7534.
94. Luo, R.; Luo, M.; Wang, Z.; Liu, P.; Song, S.; Wang, X.; Chen, M. The atomic origin of nickel-doping-induced catalytic enhancement in MoS_2 for electrochemical hydrogen production. Nanoscale 2019, 11, 7123-7128.
95. Zhang, H.; Yu, L.; Chen, T.; Zhou, W.; Lou, X.W. Surface modulation of hierarchical MoS_2 nanosheets by Ni single atoms for enhanced electrocatalytic hydrogen evolution. Advanced Functional Materials 2018, 28, 1807086.
96. Wei, S.; Cui, X.; Xu, Y.; Shang, B.; Zhang, Q.; Gu, L.; Fan, X.; Zheng, L.; Hou, C.; Huang, H. Iridium-triggered phase transition of MoS_2 nanosheets boosts overall water splitting in alkaline media. ACS Energy Letters 2018, 4, 368-374.
97. Cao, Y. Roadmap and direction toward high-performance MoS_2 hydrogen evolution catalysts. ACS nano 2021, 15, 11014-11039.
98. Jin, H.; Guo, C.; Liu, X.; Liu, J.; Vasileff, A.; Jiao, Y.; Zheng, Y.; Qiao, S.-Z. Emerging two-dimensional nanomaterials for electrocatalysis. Chemical reviews 2018, 118, 6337-6408.
99. Zhang, B.; Fan, T.; Xie, N.; Nie, G.; Zhang, H. Versatile Applications of Metal Single-Atom@2D Material Nanoplatforms. Advanced Science 2019, 6, 1901787.
100. Manzeli, S.; Ovchinnikov, D.; Pasquier, D.; Yazyev, O.V.; Kis, A. 2D transition metal dichalcogenides. Nature Reviews Materials 2017, 2, 1-15.
101. Xiong, Y.; Sun, W.; Han, Y.; Xin, P.; Zheng, X.; Yan, W.; Dong, J.; Zhang, J.; Wang, D.; Li, Y. Cobalt single atom site catalysts with ultrahigh metal loading for enhanced aerobic oxidation of ethylbenzene. Nano Research 2021, 14, 2418-2423.
102. Zhao, J.; Ji, S.; Guo, C.; Li, H.; Dong, J.; Guo, P.; Wang, D.; Li, Y.; Toste, F.D. A heterogeneous iridium single-atom-site catalyst for highly regioselective carbenoid O–H bond insertion. Nature Catalysis 2021, 4, 523-531.
103. Calle-Vallejo, F.; Loffreda, D.; Koper, M.T.; Sautet, P. Introducing structural sensitivity into adsorption–energy scaling relations by means of coordination numbers. Nature chemistry 2015, 7, 403-410.

104. Li, H.; Li, Y.; Koper, M.T.; Calle-Vallejo, F. Bond-making and breaking between carbon, nitrogen, and oxygen in electrocatalysis. Journal of the American Chemical Society 2014, 136, 15694-15701.
105. Sun, G.; Zhao, Z.-J.; Mu, R.; Zha, S.; Li, L.; Chen, S.; Zang, K.; Luo, J.; Li, Z.; Purdy, S.C. Breaking the scaling relationship via thermally stable Pt/Cu single atom alloys for catalytic dehydrogenation. Nature Communications 2018, 9, 4454.
106. Neyts, E.C.; Ostrikov, K.; Sunkara, M.K.; Bogaerts, A. Plasma catalysis: synergistic effects at the nanoscale. Chemical reviews 2015, 115, 13408-13446.
107. Yang, T.; Song, T.T.; Zhou, J.; Wang, S.; Chi, D.; Shen, L.; Yang, M.; Feng, Y.P. High-throughput screening of transition metal single atom catalysts anchored on molybdenum disulfide for nitrogen fixation. Nano Energy 2020, 68, 104304.
108. Chen, B.W.; Xu, L.; Mavrikakis, M. Computational methods in heterogeneous catalysis. Chemical Reviews 2020, 121, 1007-1048.
109. Hammer, B.; Norskov, J.K. Why gold is the noblest of all the metals. Nature 1995, 376, 238-240.
110. Li, L.; Wang, P.; Shao, Q.; Huang, X. Metallic nanostructures with low dimensionality for electrochemical water splitting. Chemical Society Reviews 2020, 49, 3072-3106.
111. Greeley, J.; Nørskov, J.K.; Mavrikakis, M. Electronic structure and catalysis on metal surfaces. Annual review of physical chemistry 2002, 53, 319-348.